Numerical Methods for the Heat Equation

Sofia Taylor, Mentored by Robert Krasny

August 2022

Contents

1 Introduction **2**
1.1 Motivation and contents . . . 2

2 Preamble **2**
2.1 Introduction to the heat equation and Fourier's derivation . . . 2
2.2 1-dimensional example . . . 3
2.3 Finite difference approximations . . . 3
2.4 Finite Precision Arithmetic . . . 5
2.5 SOR method . . . 5

3 Fourier series **6**
3.1 Steady State 1-d half infinite rod . . . 6
3.2 Steady State Half infinite (2D) bar . . . 7
3.3 Steady state temperature distribution through a finite (2D) bar . . . 9
3.4 Heat conduction through a 1D rod (time-dependent) . . . 10
3.5 Rod with nonhomogeneous boundary conditions . . . 11
3.6 Rod with insulated ends . . . 11
3.7 Dirichlet and Neumann boundary conditions . . . 13

4 Finite difference method **14**
4.1 Setup of linear system . . . 14
4.2 Solution of linear system . . . 14
4.3 Iterative Methods . . . 14
4.4 Properties of the linear system . . . 16
4.4.1 Eigenfunctions and eigenvectors . . . 17
4.4.2 Positive definite-ness . . . 18

5 Green's function **18**
5.1 Example 1 . . . 19
5.1.1 Sturm-Liouville problem . . . 20
5.1.2 Dirac Delta function . . . 20
5.1.3 Expanding the Green's function using Fourier series . . . 21
5.2 Example 2 . . . 21

6 Boundary Element Method **22**
6.1 Simple case: Square 22

7 Conclusion **24**

1 Introduction

1.1 Motivation and contents

Understanding how heat distributes throughout an object is crucial in many fields. For example, in 3D printing, nonuniform temperature distribution leads to residual stresses and deformations. The motivation for our REU project comes from a paper by Okwudire et al. [1] in which they demonstrated this effect in laboratory experiments. The goal of this project is understanding how to solve the heat equation numerically with the eventual goal of simulating the experiments in [1].

The report is organized as follows. Section 2 is a preamble which introduces the heat equation and gives the derivation, as well as some background for the numerical methods we will use. Section 3 will introduce Fourier series expansions and use them to solve many different heat conduction problems. Section 4 solves a particular problem using the finite difference method, and section 5 introduces Green's functions and integral relationships that result from the heat equation. We attempt to numerically solve the heat equation using these integral relations. Many thanks to Robert Krasny for his wonderful mentorship and insight throughout this project.

2 Preamble

We first introduce the temperature function $u(x, y, z, t)$ at a point in space, (x, y, z) at time t (the words temperature and heat will be used almost interchangeably throughout this paper). Often it is simpler and more helpful to reduce to a function of only 1 or 2 spatial variables, looking at thin rods or flat surfaces. Removing the time dependence allows us to look at what are called steady state problems. Another important concept associated with the heat function is the heat flux, also called the normal derivative, which can be thought of as the flow of heat through a surface. All of these terms will be defined more in depth as they arise throughout the paper.

2.1 Introduction to the heat equation and Fourier's derivation

In 1807, Joseph Fourier published his book, "The Analytical Theory of Heat," where he presented his derivation of the heat equation and a solution in terms of trigonometric series. Below is the derivation almost as Fourier presented as well as an intuitive interpretation.

Start by considering the cube in Figure 1, with dimensions dx, dy, dz, which shows that in a time interval dt the heat flux through the left face is $dy\,dz\,\dfrac{du}{dx}\,dt$ and through the right face is $dy\,dz\,\dfrac{du}{dx}\,dt - dy\,dz\,d(\dfrac{du}{dx})\,dt$. Then the contribution to the heat in the volume due to the flux through the left and right faces is $dy\,dz\,\dfrac{du}{dx}\,dt - \left(dy\,dz\,\dfrac{du}{dx}\,dt - dy\,dz\,d(\dfrac{du}{dx})\,dt\right) =$

$dy\,dz\,d(\frac{du}{dx})\,dt \approx dy\,dz\,\frac{d^2u}{dx^2}\,dx\,dt$, and a similar relation follows by permuting the variables.

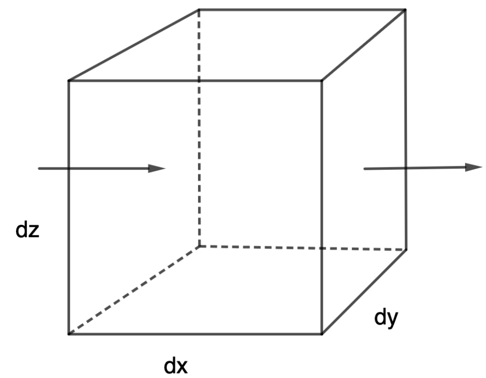

Figure 1: We begin with a cube of volume $dV = dx\,dy\,dz$, so small that the temperature remains constant across a single face. The flux through one face, assuming flux is constant across the face, is given by the rate of temperature change across the face multiplied by the area of the face. Conductivity constants are all set to 1 for simplicity.

Then, by conservation of energy, the heat energy in the cube is given by

$$du\,dV = [\text{flux into } V \text{ through 3 faces}] - [\text{flux out of } V \text{ through the opposite 3 faces}] \tag{1}$$

$$du\,dV = dy\,dz\,d(\frac{du}{dx})\,dt + dz\,dx\,d(\frac{du}{dy})\,dt + dy\,dx\,d(\frac{du}{dz})\,dt \tag{2}$$

$$= dx\,dy\,dz\,(\frac{d^2u}{dx^2} + \frac{d^2u}{dy^2} + \frac{d^2u}{dz^2})\,dt \tag{3}$$

$$\frac{du}{dt} = \frac{d^2u}{dx^2} + \frac{d^2u}{dy^2} + \frac{d^2u}{dz^2} = \Delta u \tag{4}$$

With the heat conductivity proportionalities included, this becomes:

$$\alpha^2 u_t = u_{xx} + u_{yy} + u_{zz}$$

For simplicity, all calculations in this paper are done using the heat equation (4). The next subsection considers a 1-dimensional example.

2.2 1-dimensional example

The example in figure 2 can give some quick intuition on the heat equation.

In 1D, the heat equation looks like $u_t = u_{xx}$. This tells us that if the function is concave down at a certain point, then the temperature must decrease over time. Similarly, if the function is concave up at a certain point, then the temperature must increase with time.

As $t \to \infty$, the temperature stops changing over time. The equation becomes $0 = u_{xx}$, or, more generally, $0 = \Delta u$. This is called the *steady state*. The steady state solution for the problem above is $u = 0$.

2.3 Finite difference approximations

Finite difference approximations are used to approximate derivatives on a discrete meshgrid. To begin, we discretize the domain. In 1D, the discretization is given in figure 3.

The approximation for the first derivative, which we will not derive, is given by:

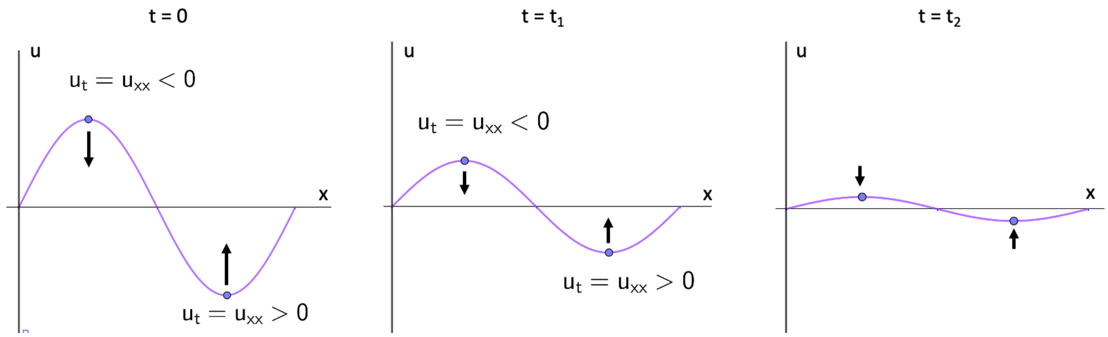

Figure 2: A finite 1-dimensional rod with an initial sinusoidal temperature distribution has ends held at zero degrees.

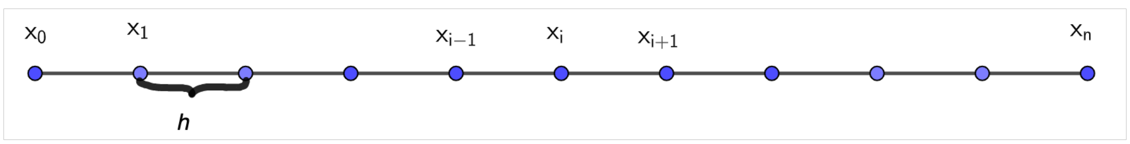

Figure 3: $x_i = ih$: meshpoints, $i = 0 : n$, h: mesh spacing

$$\frac{f(x+h) - f(x)}{h} = f'(x) + \frac{1}{2}f''(x)h + \ldots$$

where the error is given by the truncation error:

$$\frac{1}{2}f''(x)h + \ldots$$

which is of order $O(h)$.

After we discretize, we can either take the forward difference:

$$D_+f = \frac{f(x_{i+1}) - f(x_i)}{h}, \tag{5}$$

or the backwards difference:

$$D_-f = \frac{f(x_i) - f(x_{i-1})}{h}. \tag{6}$$

To approximate the 2nd derivative, we use Taylor expansions about x_i, where ξ is some value between 0 and x:

$$f(x) = f(x_i) + f'(x_i)(x - x_i) + \frac{f''(x_i)}{2}(x - x_i)^2 + \frac{f'''(\xi(x))}{6}(x - x_i)^3$$

$$f(x_{i+1}) = f(x_i + h) = f(x_i) + hf'(x_i) + h^2\frac{f''(x_i)}{2} + h^3\frac{f'''}{6}\ldots$$

$$f(x_{i-1}) = f(x_i - h) = f(x_i) - hf'(x_i) + h^2\frac{f''(x_i)}{2} - h^3\frac{f'''}{6}\ldots$$

$$f(x_{i+1}) + f(x_{i-1}) = 2f(x_i) + h^2f''(x_i) + \frac{h^4}{4!}(f''') + \ldots$$

When the x_is are close, h is very small, the following becomes a good approximation with error of order $O(h^2)$

$$f''(x_i) \approx \frac{f(x_{i+1}) - 2f(x_i) + f(x_{i-1})}{h^2} \tag{7}$$

Note that this is also $D_+(D_-f)$.

2.4 Finite Precision Arithmetic

Using Matlab, we will do a brief error analysis of the first derivative finite difference approximation. Using either equations (5) or (6), we will approximate the derivative of e^x, which we know to be e^x. In theory, as we decrease h, the error should decrease as $O(h)$. However, due to finite precision arithmetic, this is not the case computationally.

In figure 4, we plot the error against h. As h decreases, the error decreases as expected until $h \approx 10^{-8}$. This is where the truncation error dominates. The error begins to increase when the roundoff error from finite precision arithmetic (which is of order $O(\epsilon/h)$) dominates over the truncation error.

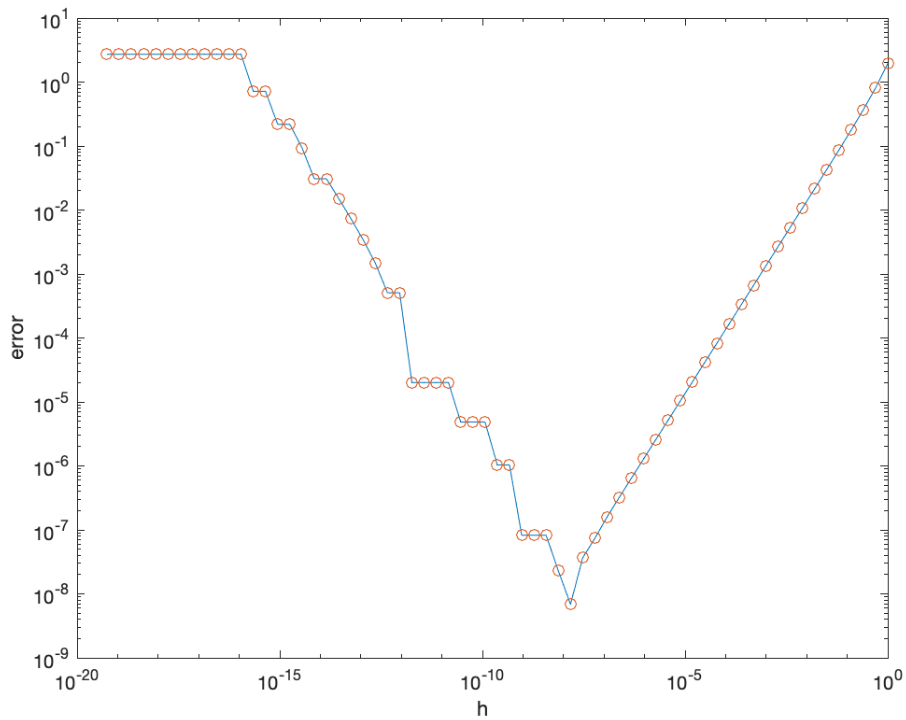

Figure 4: Error $|D_+(e^x) - e^x|$ vs. Mesh Spacing

2.5 SOR method

To solve a linear system $Ax = b$, one technique is to use a fixed point iterative method by rewriting the system as an equivalent system: $x = Tx + c$. There are many different ways to define T. The SOR method of defining T is described below:

First, we let $A = D - L - U$, where D is the diagonal, $-L$ is the strictly lower triangular part of A, and $-U$ the strictly upper part of A. We can begin to rearrange $Ax = b$:

$$\begin{aligned} Ax = b &\Rightarrow (D - L - U)x = b \\ &\Rightarrow (\omega D - \omega L - \omega U)x = \omega b \\ &\Rightarrow (D - (1-\omega)D - \omega L - \omega U)x = \omega b \\ &\Rightarrow (D - \omega L)x = [(1-\omega)D + \omega U]x + \omega b \\ &\Rightarrow x = (D - \omega L)^{-1}[(1-\omega)D + \omega U]x + (D - \omega L)^{-1}\omega b \end{aligned}$$

This is now in the form of $x = Tx + c$. If we do some rearranging, we see:

$$\Rightarrow x^{(k+1)} = (1-\omega)x^k + \omega D^{-1}[Lx^{(k+1)} + Ux^{(k)} + b]$$

The second term is the Gauss-Seidel iteration, meaning this method is essentially a "weighted average," or more precisely, an affine combination, of the new Gauss-Seidel value with the one obtained during the previous iteration. Here ω is the so-called relaxation parameter. If $\omega = 1$ we simply have the Gauss-Seidel method.

3 Fourier series

We will begin with using Fourier series to solve the heat equation on certain domains with certain boundary conditions.

3.1 Steady State 1-d half infinite rod

Before we look at more complicated heat distributions, our first example is the steady state half-infinite, thin rod as depicted in figure 5.

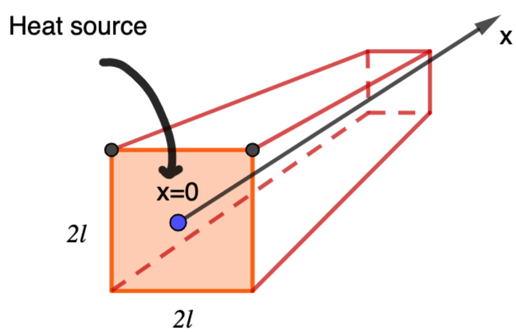

Figure 5: Half-Infinite rod with square cross section of width $2l$, $l << 1$ with a heat source at $x = 0$. As $t \to \infty$.

At the steady state, during one time unit, the heat that passes through a cross section of width dx must be equal to the heat escaping through the surface of that cross section:

Let h and k be the internal and external conducibility. The above statements can now be formulated into the following equations:

$$-4l^2 k \frac{du}{dx} = \int_0^\infty 8hlu(x)dx - \int_0^x 8hlu(x)dx$$

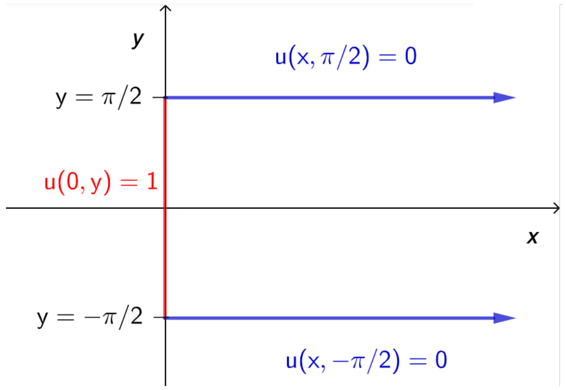

Figure 6: Domain and Boundary Conditions

$$kl\frac{d^2u}{dx^2} = 2hu$$

$$u = Ae^{-x\sqrt{\frac{2h}{lk}}} + Be^{x\sqrt{\frac{2h}{lk}}}$$

To solve for the constants A and B, we use

$$lim_{x\to\infty}u(x) = 0 \implies B = 0$$

A can be solved for given any additional boundary point value.

3.2 Steady State Half infinite (2D) bar

We will be solving the steady state heat equation on the domain pictured in figure 6 with the problem stated as follows:

Domain: $(x,y) \in [0,\infty) \times [-\pi/2, \pi/2]$

Boundary Conditions: $u(0,y) = 1$, $u\left(x, \pm\frac{\pi}{2}\right) = 0$, $\lim_{x\to\infty} u(x,y) = 0$.

$$\frac{\partial^2 u}{\partial x^2} + \frac{\partial^2 u}{\partial y^2} = 0$$

Note that one of our "boundary" conditions is at infinity.

We begin solving with separation of variables, assuming the solution is in the form $u(x,y) = X(x)Y(y)$. With this assumption, we find the following special solutions that satisfy boundary conditions at $x = \pm\frac{\pi}{2}$:

$$u_n(x,y) = e^{-(2n+1)x}\cos(2n+1)y, n = 0,1,2,3,\ldots$$

By linearity, we know a linear combination of solutions is still a solution, so we can look for a solution in the form of: $u(x,y) = \sum_{n=0}^{\infty} a_n u_n(x,y)$. To solve for the constants, we apply the boundary conditions:

$$x = 0 \Rightarrow u(0,y) = 1 \Rightarrow 1 = \sum_{n=0}^{\infty} a_n \cos(2n+1)y$$

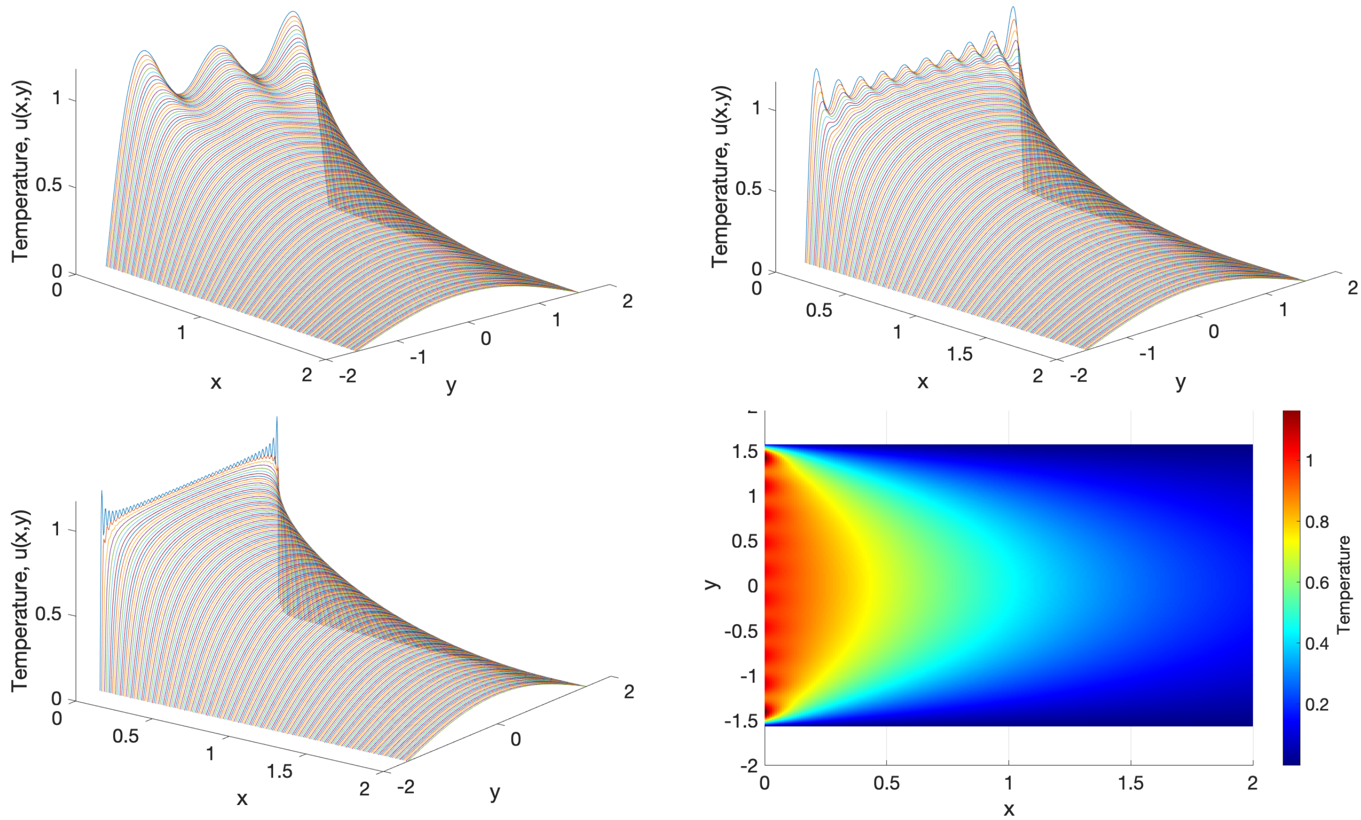

Figure 7: Temperature distribution through a half-infinite bar of width π, calculated on a meshgrid using the first m nonzero terms of the fourier series given in equation 8.
Upper left: $m = 3$, Upper right: $m = 10$, lower left: $m = 50$, lower right: contour plot using $m = 10$
.

$$\int_{-\frac{\pi}{2}}^{\frac{\pi}{2}} 1 \cdot \cos(2n+1)y \; dy = \int_{-\frac{\pi}{2}}^{\frac{\pi}{2}} \sum_{n=0}^{\infty} a_n \cos(2n+1)y \cdot \cos(2n+1)y \; dy$$

$$\Rightarrow a_n = \frac{4(-1)^n}{(2n+1)\pi}$$

The Fourier series for the solution of the heat equation is

$$u(x,y) = \sum_{n=0}^{\infty} \frac{4(-1)^n}{(2n+1)\pi} e^{-(2n+1)x} \cos(2n+1)y. \tag{8}$$

To evaluate this numerically, we have to truncate the infinite sum and then evaluate. Figure 7 shows the heat distribution through a finite 2D bar with different truncations. Note the non-uniform convergence at the corners. This is known as Gibbs Phenomenon and occurs at discontinuities like corners.

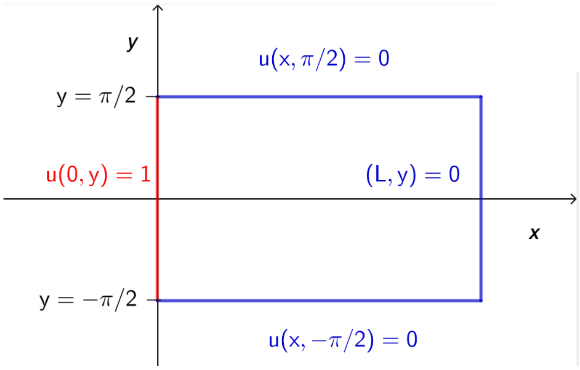

Figure 8: Domain and boundary conditions

3.3 Steady state temperature distribution through a finite (2D) bar

We now introduce a problem to which we will return and solve with each method presented in the paper. Similar to the previous problem in section 3.2, we solve the steady state heat equation but now on a finite domain shown in figure 8:

Domain: $(x, y) \in [0, L] \times [-\pi/2, \pi/2]$

Boundary Conditions: $u(0, y) = 1$, $u\left(x, \pm\frac{\pi}{2}\right) = 0$, $u(L, y) = 0$

$$\frac{\partial^2 u}{\partial x^2} + \frac{\partial^2 u}{\partial y^2} = 0$$

.

The same method can be applied and we reach the solution:

$$u(x, y) = \sum_{n=1,3,5}^{\infty} \frac{(-1)^{\frac{n-1}{2}} * 4}{n\pi(1 - e^{2nL})}(e^{nx} - e^{2nL-nx})\cos(ny)$$

note that, as we take L to infinity this turns into equation 8. The solution is depicted in figure 9.

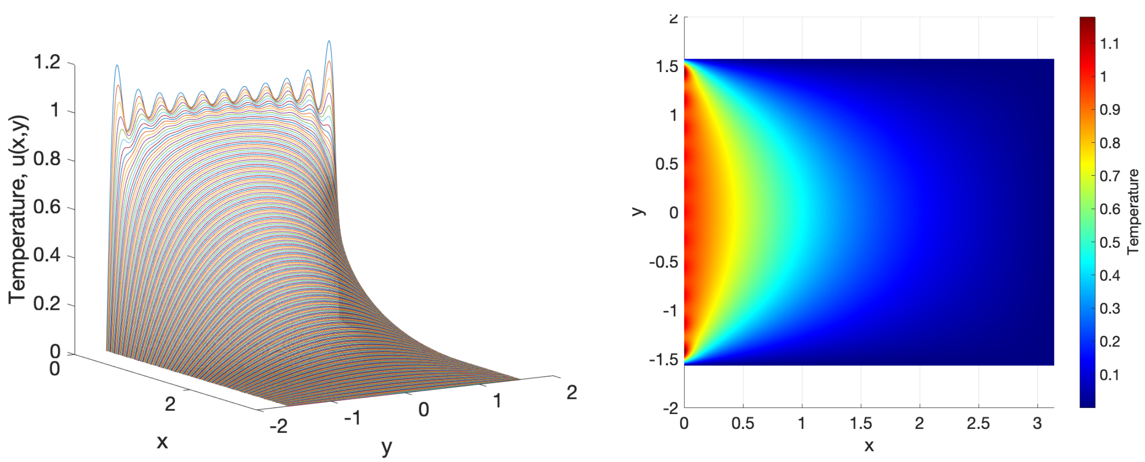

Figure 9: The steady state solution through a finite square of length π. The figures are plotted by evaluating the Fourier series solution truncated at 10 terms. On the right is a contour plot.

In the next section, we will move away from steady state problems and introduce the time variable t.

3.4 Heat conduction through a 1D rod (time-dependent)

We now introduce time dependent problems with one spatial variable. To solve these problems, we need boundary conditions as well as an initial temperature distribution at $t = 0$.

We solve the 1D heat equation,

$$\frac{\partial}{\partial t}u(x,t) = \frac{\partial^2}{\partial t^2}u(x,t),$$

on a finite rod of length L that has the following initial conditions and homogeneous boundary conditions:

-initial uniform temperature distribution given: $u(x,0) = f(x)$

-homogeneous case: $u(0,t) = 0, u(L,t) = 0$

Using separation of variable again, we come across a very similar process as in the previous examples. The solution must be a linear combination of the following special solutions:

$$u(x,t) = \sum_{n=1}^{\infty} c_n e^{-n^2\pi^2 t/L} \sin\frac{n\pi x}{L}$$

and after applying the rest of the boundary conditions:

$$u(x,0) = f(x) \implies c_n = \frac{2}{L}\int_0^L f(x)\sin\frac{n\pi x}{L}dx$$

The solution with $L = \pi$ and initial temperature distribution, $u(x,0) = c$ is given by the following equation:

$$u(x,t) = \sum_{n=1,3,5...}^{\infty} \frac{4c}{n\pi} e^{-n^2\pi t}\sin(nx) \tag{9}$$

and depicted in figure 10.

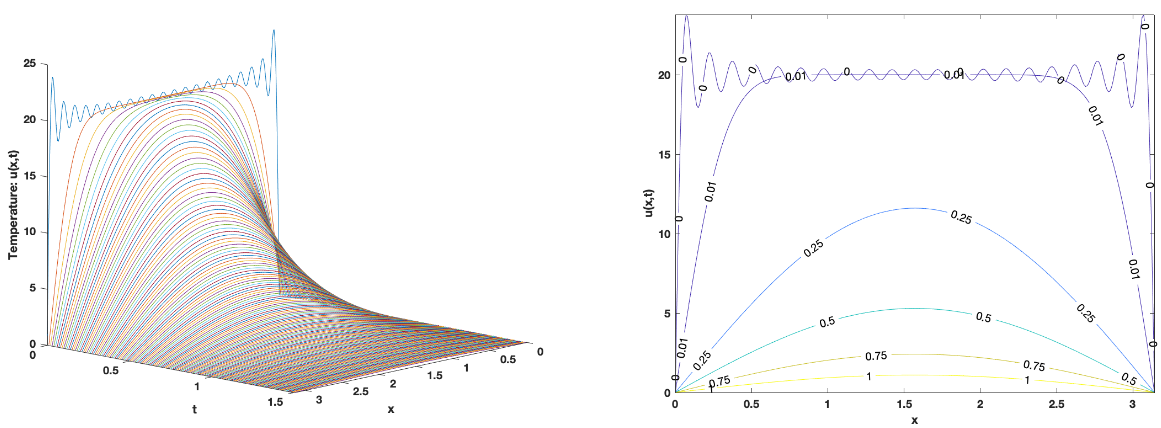

Figure 10: Time-dependent heat equation, finite rod with homogeneous boundary conditions on $0 \le x \le \pi$ with constant initial temperature $c = 20$, calculated using the first 20 nonzero partial sums of the Fourier series in equation (9). Left: $u(x,t)$ Each curve represents the temperature distribution at a certain time. Plotting all of the curves together as time extends along one axis gives a surface plot. Right: $u(x,t)$ as contour plot where each contour represents temperature distributions at specific times t, as indicated on the plot.

In the next section, we look at a slightly more complicated case. The temperature is still specified at each end, but is nonzero.

3.5 Rod with nonhomogeneous boundary conditions

In general, when the boundary is held at constant temperature, this is called Dirichlet boundary conditions. The previous example was a special case: homogeneous Dirichlet boundary conditions. In this example, we have nonhomogenous Dirichlet boundary conditions given by:

$$u(0,t) = t_1, u(L,t) = t_2.$$

We are again given an initial distribution:

$$u(x,0) = f(x).$$

First, we reduce the problem to a homogeneous problem by subtracting the steady state solution. In equation (10), the steady state solution is the linear term before the sum. Then, the solution follows exactly as in the previous example and is given by the summation.

$$u(x,t) = (T_2 - T_1)\frac{x}{L} + T_1 + \sum_{n=1}^{\infty} c_n e^{-n^2\pi^2 t/L} \sin\frac{n\pi x}{L} \tag{10}$$

$$u(x,0) = f(x) \implies c_n = \frac{2}{L}\int_0^L (f(x) - (T_2 - T_1)\frac{x}{L} - T_1) \sin\frac{n\pi x}{L} dx \tag{11}$$

To model a concrete example, we begin with a rod of length π with initial temperature distribution $f(x) = 20$ and boundary conditions $u(x,t) = 20$, $u(\pi,t) = 100$.

The solution is given by:

$$u(x,t) = (80)\frac{x}{\pi} + 20 + \sum_{n=1}^{\infty} \frac{160 * (-1)^n}{n\pi} e^{-n^2\pi t} \sin(nx) \tag{12}$$

and is depicted in figure 11.

Note the similarities between equation (12) and equation (9).

In the following example, we introduce a new kind of boundary condition given by the flux on the boundary.

3.6 Rod with insulated ends

Suppose we no longer know the temperature at the ends of our rod, but we do know how much heat escapes from the ends. This type of boundary condition is called a Neumann boundary condition and is given by fixing $u_x(0,t)$ and $u_x(L,t)$.

The solution is found in much the same way as the Dirichlet problem with separation of variables, however we end up solving a slightly different eigenfunction problem.

If we begin with initial temperature distribution $u(x,0) = f(x)$ and Neumann conditions $u_x(0,t) = u_x(L,t) = 0$, we reach the follow special solutions:

$$u(x,t) = \frac{c_0}{2} + \sum_{n=1}^{\infty} c_n e^{-n^2\pi^2 t/L} \cos\frac{n\pi x}{L}$$

Applying the initial distribution, we arrive at the solution:

$$u(x,0) = f(x) \implies c_n = \frac{2}{L}\int_0^L f(x) \cos\frac{n\pi x}{L} dx.$$

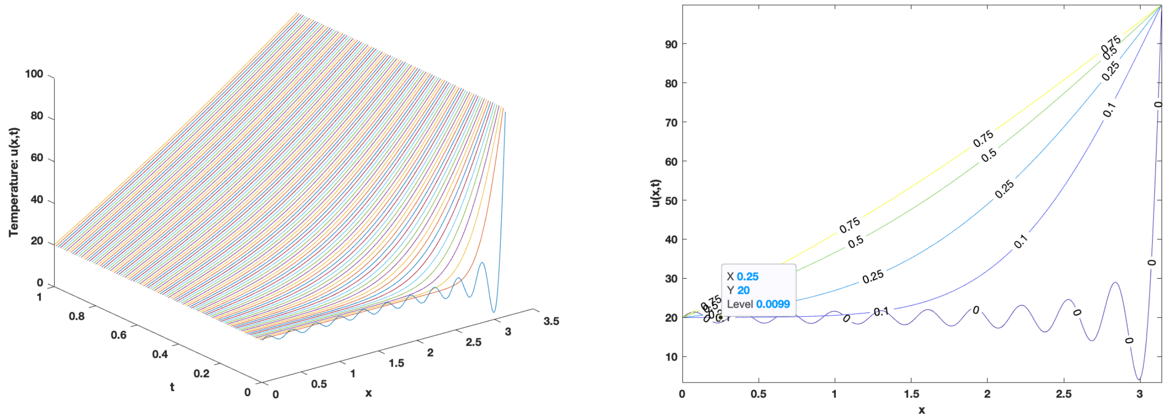

Figure 11: Time-dependent heat equation, finite rod with nonhomogeneous Dirichlet boundary conditions on $0 \le x \le \pi$ with constant initial temperature $c = 20$, calculated using the first 20 nonzero partial sums of the Fourier series in equation (12). Left: $u(x,t)$ as a surface plot, Right: $u(x,t)$ as a contour plot. Notice that Gibbs phenomenon only appears on the right end of the rod. This is because there is no discontinuity on the left end as it starts and remains at Temperature 20.

We model an example for a rod of length $L = \pi$, initial distribution $u(x,0) = x$. The solution is:

$$u(x,t) = \frac{\pi}{2} - \sum_{n=1}^{\infty} \frac{4}{n^2\pi} e^{-n^2 t} \cos nx \tag{13}$$

and is depicted in figure 12.

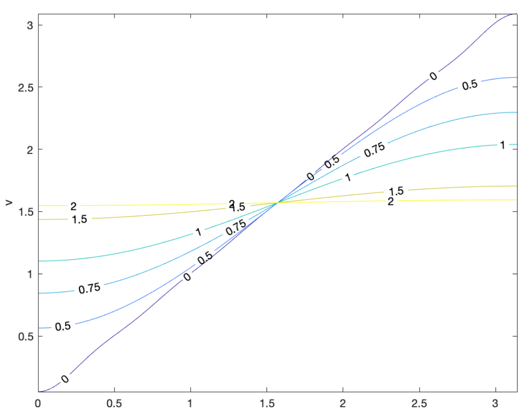

Figure 12: Time-dependent heat equation, finite rod with homogeneous Neumann boundary conditions (insulated ends) on $0 \le x \le \pi$ with initial distribution $u(x,0) = x$, calculated using the first 20 nonzero partial sums of the Fourier series in equation (13). $u(x,t)$ as a contour plot. Notice that there is no Gibbs phenomenon and the series converges rapidly.

In the following example, we see a problem with mixed boundary conditions.

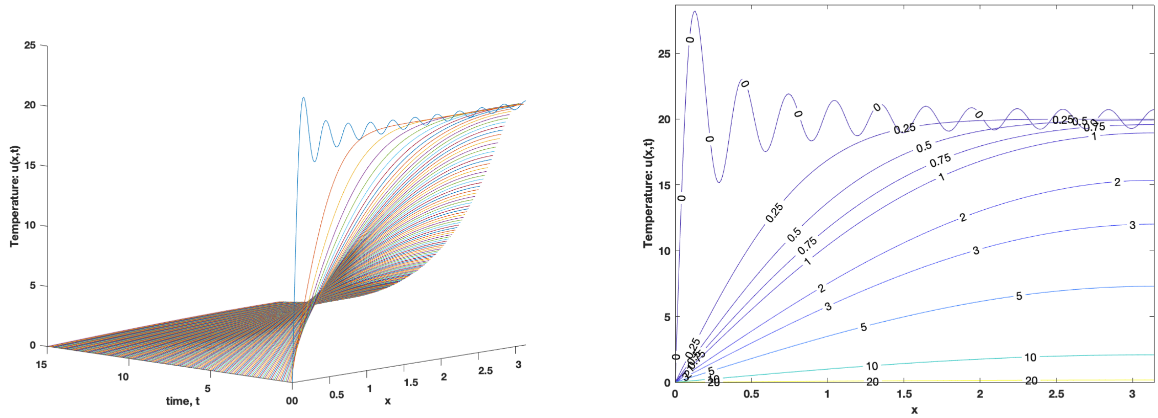

Figure 13: Time-dependent heat equation, finite rod with one insulated end and one end held at Temperature 0 on $0 \le x \le \pi$ with initial distribution $u(x,0) = 20$, calculated using the first 20 nonzero partial sums of the Fourier series in equation (14). Left: $u(x,t)$ as a surface plot, Right: $u(x,t)$ as a contour plot. Notice that there is no Gibbs phenomenon on the right side of the rod.

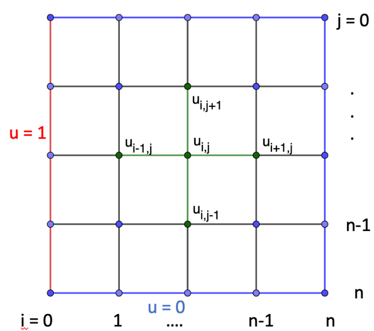

Figure 14: The discretized domain and it's boundary conditions

3.7 Dirichlet and Neumann boundary conditions

Suppose we hold only one end at constant temperature and we control the heat that escapes out of the other end. This is now a mixed Dirichlet-Neumann problem.

We look at a simple case, where one end is held at constant temperature $u(0,t) = 0$ and the other end fully insulated: $u_x(L,t) = 0$, again with constant initial distribution $u(x,0) = c$. The solution is given by the following:

$$u(x,t) = \sum_{n=1,3,5\ldots}^{\infty} \frac{4c}{n\pi} e^{-n^2 t/4} \sin(\frac{n}{2}x) \tag{14}$$

and is depicted in figure 13

$$
\left(\begin{array}{ccc|ccc|ccc}
4 & -1 & & -1 & & & & & \\
-1 & 4 & -1 & & -1 & & & & \\
 & -1 & 4 & & & -1 & & & \\
\hline
-1 & & & 4 & -1 & & -1 & & \\
 & -1 & & -1 & 4 & -1 & & -1 & \\
 & & -1 & & -1 & 4 & & & -1 \\
\hline
 & & & -1 & & & 4 & -1 & \\
 & & & & -1 & & -1 & 4 & -1 \\
 & & & & & -1 & & -1 & 4
\end{array}\right)
\begin{pmatrix} u_{1,1} \\ u_{2,1} \\ u_{3,1} \\ u_{1,2} \\ u_{2,2} \\ u_{3,2} \\ u_{1,3} \\ u_{2,3} \\ u_{3,3} \end{pmatrix}
=
\begin{pmatrix} 1 \\ 0 \\ 0 \\ 1 \\ 0 \\ 0 \\ 1 \\ 0 \\ 0 \end{pmatrix}
$$

Figure 15: matrix set up for a 3×3 discretization

4 Finite difference method

4.1 Setup of linear system

To solve the steady state problem of the finite bar, as first presented and described in section 3.3, we can discretize the domain and approximate the solution using the finite difference approximations derived and explained in section 2.3.

A reminder of the problem: we want to solve the Laplace equation, $u_{xx} + u_{yy} = 0$ on the domain $(x, y) \in (0, L) \times (-\frac{L}{2}, \frac{L}{2})$ with the following boundary conditions: $u(0, y) = 1$, $u(x, \pm\frac{L}{2}) = u(L, y) = 0$.

We begin by discretizing the domain, as seen in figure 14. Using the approximations $u_{xx} \approx D_+^x D_-^x u_{i,j}$ and $u_{yy} \approx D_+^y D_-^y u_{i,j}$, we can rewrite the Laplace equation as follow:

$$D_+^x D_-^x u_{i,j} + D_+^y D_-^y u_{i,j} = 0 \tag{15}$$

$$\frac{u_{i+1,j} - 2u_{i,j} + u_{i-1,j}}{h^2} + \frac{u_{i,j+1} - 2u_{i,j} + u_{i,j-1}}{h^2} = 0 \tag{16}$$

$$u_{i+1,j} + u_{i-1,j} - 4u_{i,j} + u_{i,j+1} + u_{i,j-1} = 0 \tag{17}$$

We want to solve for $u_{i,j}$ at every point (i, j). We can represent this as a system of linear equations $Ax = b$, where the entries of A are the coefficients of equation 17, the vector x is the $u_{i,j}s$, the solution to our heat equation at discretized points along a grid, and our boundary conditions are contained in the right-hand side in b. In the 3×3 example, the set up is shown in figure 15.

4.2 Solution of linear system

The solution, obtained using the SOR method outlined in section 2.5, on a 1×1 square with $h = 1/16$ is shown in figure 16.

4.3 Iterative Methods

To solve the system, we can use iterative methods. Figure 17 compares the convergence rates of the Jacobi, Gauss-Seidel, and SOR iterative method. Recall that the SOR method and the Gauss-Seidel method was outlined in section 2.5. The convergence rate of each iterative

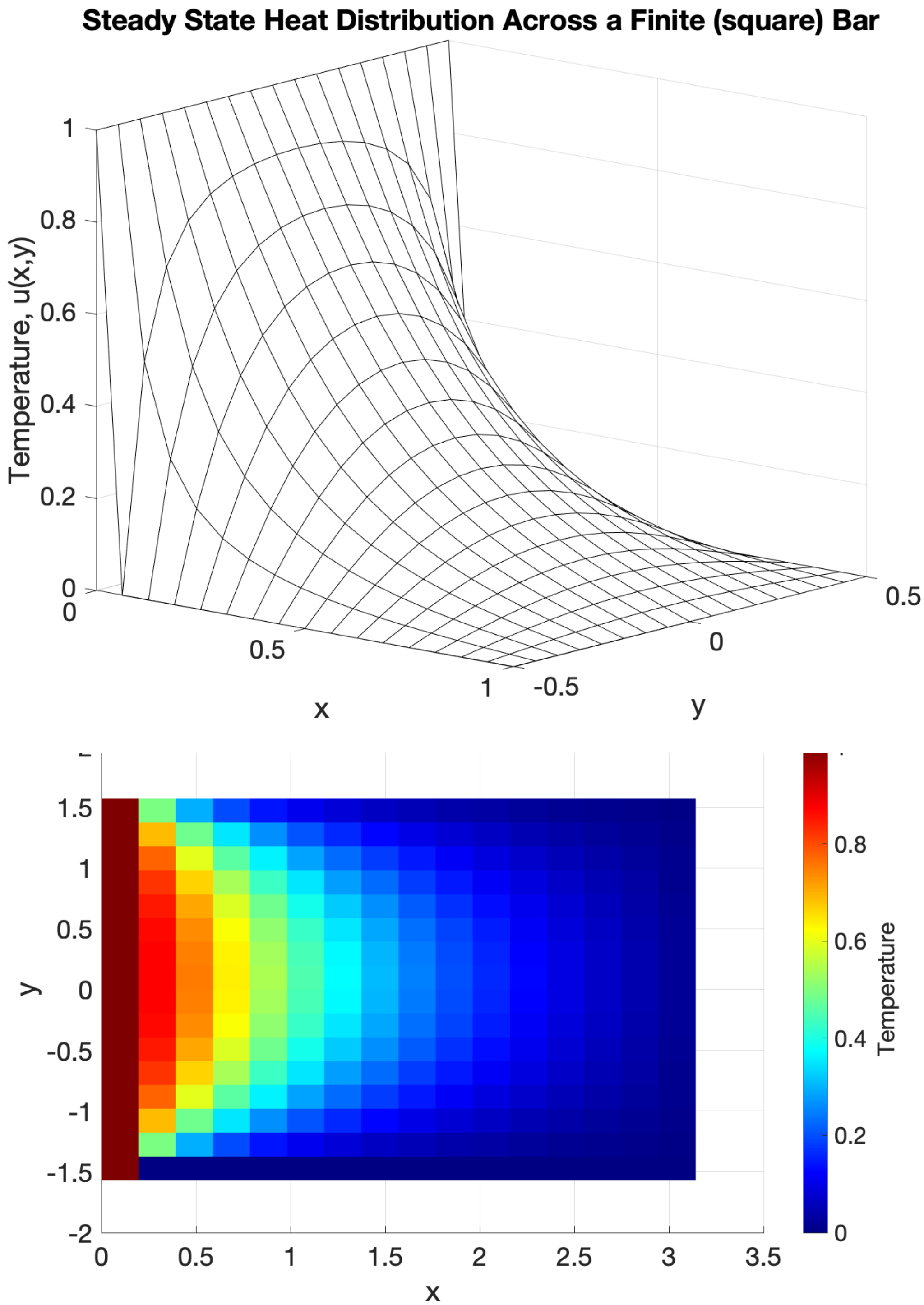

Figure 16: Solution to the steady state heat equation on a 2D square bar, given by finite difference method. Top: surface plot with temperature on the Z-axis. Bottom: colormap of the solution.

methods is determined by the spectral radius of the iteration matrix. The results show that, for each method, the convergence rate decreases as the meshgrid is refined. Additionally, we see that Gauss-Seidel converges faster than Jacobi, and SOR faster than Gauss-Seidel.

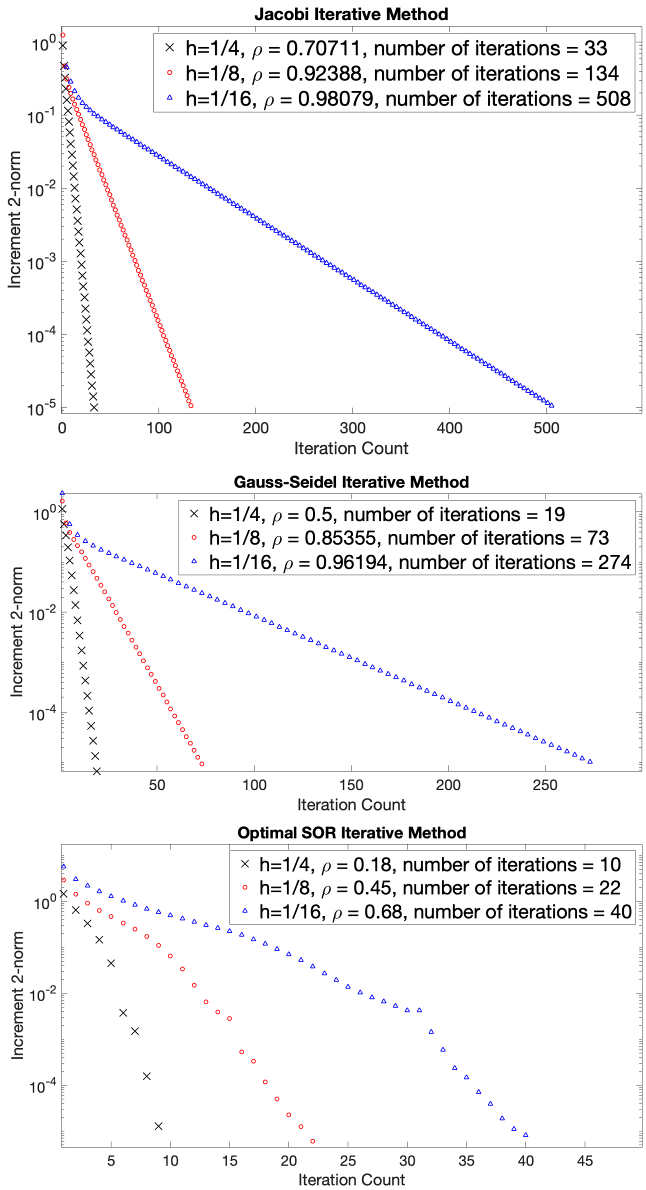

Figure 17: Convergence rates of respective iterative methods for different meshgrids. The legend includes the spectral radius of each iteration matrix as well as the number iterations until convergence (note the correlation between the two).

4.4 Properties of the linear system

We will now examine some properties of the matrix in both 1D and 2D.

4.4.1 Eigenfunctions and eigenvectors

We want to see how the eigenfunctions of the linear operator Laplace operator compare with the eigenvectors of the matrix in the discrete case. Let's begin with the 1D case: $-y'' = f(x)$ BC: $y(0) = y(1) = 0$, where $\mathcal{L}(y) = -y''$. Discretize so that we have n interior points. Finite difference approximation gives us a matrix that looks like:

$$A = \begin{bmatrix} 2 & -1 & 0 & 0 & 0 & 0 \\ -1 & 2 & -1 & 0 & 0 & 0 \\ 0 & \cdot & \cdot & . & 0 & 0 \\ 0 & 0 & \cdot & \cdot & \cdot & 0 \\ 0 & 0 & 0 & \cdot & & -1 \\ 0 & 0 & 0 & 0 & -1 & 2 \end{bmatrix}$$

Recall that the eigenfunctions of the differential linear operator $\mathcal{L}(y)$, given by $\mathcal{L}(y) = \lambda y$, are:

$$y = a_1 \sin(nx) + a_2 \cos(nx) \tag{18}$$

After applying the boundary conditions, we see that $a_2 = 0$ and $n = k\pi$, where $k = 1, 2, 3....$ Our eigenfunctions are then:

$$y_k(x) = \sin(\pi x), \sin(2\pi x), \sin(3\pi x), ... \tag{19}$$

The hypothesis is that the eigenfunctions evaluated on the mesh points are the eigenvectors of the matrix. This can be shown as follows: If we evaluate these eigenfunctions on our mesh points ($x_j = j \cdot L/(n+1) = j \cdot h$), for a given $j = 1 : n$, we get the vectors:

$$\mathbf{v}_k = [v_{k,j}] = [y_k(x_j)] = [\sin(k\pi h), \ldots, \sin(k\pi jh), \ldots, \sin(k\pi nh)]^T$$

To verify that these are eigenvectors, we compute $A\mathbf{v}_k$:

$$[A\mathbf{v}_k]_j = -1 \cdot \sin(k\pi(j-1)h) + 2 \cdot \sin(k\pi jh) - 1 \cdot \sin(k\pi(j+1)h) \tag{20a}$$
$$= (\sin(k\pi jh))(2 - 2\cos(k\pi h)), \tag{20b}$$
$$= [\mathbf{v}_k]_j (2 - 2\cos(k\pi h)) \tag{20c}$$

where it should be noted that equation (20a) is true even for $[Av_k]_1$ and $[Av_k]_n$ because the first term evaluates to zero when $j = 1$ and so does the last term when $j = n$, and equation (20b) follows using the angle addition formulas. Note equation (20c) follows because the j^{th} component of v_k is given by $v_{k,j} = \sin(k\pi jh)$, so it is indeed an eigenvector with eigenvalue $\lambda_k = 2 - 2\cos(k\pi h)$. Additionally, by taking k from 1 to n, we see that the matrix has n distinct and nonzero eigenvalues, verifying that the matrix is invertible. This property can be extended to the 2D case.

4.4.2 Positive definite-ness

Another property that the (minus) Laplacian operator has is that it is positive definite. In this section, we show that the matrix of the discrete representation is also positive definite. Positive-definiteness also implies invertibility, a property we want to make sure our matrix has. To prove positive definite-ness, we show that $x^t[Ax] > 0$ for any nonzero x.

In the simple, 1D case:

$$\begin{aligned} x^t[Ax] &= \sum_{i=1}^{n} x_i(-x_{i-1} + 2x_i - x_{i+1}) \\ &= x_1(2x_1 - x_2) + \left(\sum_{i=2}^{n-1} x_i(-x_{i-1} + 2x_i - x_{i+1}) \right) + x_n(2x_n - x_{n-1}) \end{aligned}$$

Which can be rewritten as:

$$= x_1^2 + \left(\sum_{i=1}^{n-1} (x_i - x_{i+1})^2 \right) + x_n^2 > 0 \text{ for any nonzero x. } \blacksquare$$

We can similarly extend this property to the 2D case:

$$x = \begin{bmatrix} [x_1] \\ \vdots \\ [x_n] \end{bmatrix}, \quad A = \begin{bmatrix} T & -I & & & \\ -I & T & -I & & \\ & \cdot & \cdot & \cdot & \\ & & \cdot & \cdot & \cdot \\ & & & -I & T \end{bmatrix}, \quad T = \begin{bmatrix} 4 & -1 & & & \\ -1 & 4 & -1 & & \\ & \cdot & \cdot & \cdot & \\ & & \cdot & \cdot & \cdot \\ & & & -1 & 4 \end{bmatrix}$$

Where there are $n \times n$ interior points in the domain, x is partitioned into "block vectors" of length n, and I and T are $n \times n$.

$$x^t[Ax] = x_1^T T x_1 - x_1^T x_2 + \sum_{j=2}^{n-1} (-x_j^T x_{j-1} + x_j^T T x_j - x_j^T x_{j+1}) + x_n^T T x_1 n - x_n^T x_{n-1} \tag{21}$$

Note that, by Gershgorin circle theorem, all the eigenvalues of T are between 2 and 6 inclusive, so we have the following inequality:

$$x_j^T T x_j \geq 2 x_j^T x_j = 2|x_j|^2$$

Using this inequality, equation 21 satisfies the inequality

$$x^t[Ax] \geq |x_1|^2 + \sum_{j=1}^{n-1} (|x_i - x_{i+1}|^2) + |x_n|^2 > 0 \text{ for any nonzero x. } \blacksquare \tag{22}$$

In the following section, we introduce a third way to solve the heat equation.

5 Green's function

If we extend the linear algebra analogy, where Fourier series solutions are the eigenfunction expansion of the solution (similar to eigenvector expansions when solving a linear system), then Green's functions would be analogous to the inverse of the linear system, applicable to any right hand side. The laborious calculations will be left out in the following example.

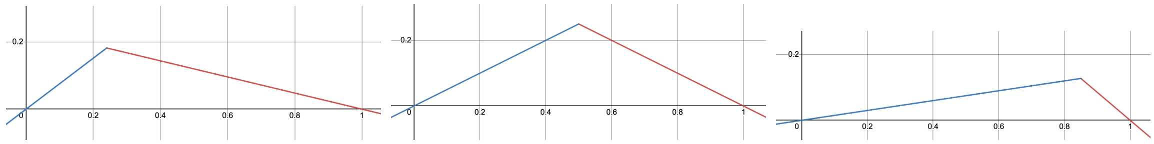

Figure 18: Green's function for different values of s (from left to right: $s = 0.25$, $s = 0.5$, $s = 0.8$

5.1 Example 1

We start with a simple problem in 1D:

$$-y''(x) = f(x)$$

.

This can be thought of as a steady state heat problem, where the $f(x)$ on the right side represents some heat source beneath a rod.

To solve this with variation of parameters, we would first find the fundamental solutions to the homogeneous equation, $y_1 = 1$, $y_2 = x$.

Then, using variation of parameters, we find a particular solution Y:

$$\begin{aligned} Y &= -y_1 \int_0^x \frac{y_2 f(s)}{W[y_1, y_2]} ds + y_2 \int_0^x \frac{y_1 f(s)}{W[y_1, y_2]} && (23) \\ &= \int_0^x (x - s) f(s) ds && (24) \end{aligned}$$

The general solution is then given by:

$$\phi(x) = c_1 + c_2 x + \int_0^x (x - s) f(s) ds. \tag{25}$$

When given boundary conditions $y(0) = 0$, $y(1) = 0$, we can rearrange and write the solution as:

$$\phi(x) = \int_0^1 G(x, s) f(s) ds \tag{26}$$

where

$$G(x, s) = \begin{cases} s(1 - x) & \text{if } 0 \le s \le x \\ x(1 - s) & \text{if } x \le s \le 1 \end{cases} \tag{27}$$

The Green's function is depicted for different values of s in figure 18. The solution is given as a definite integral of the Green's function multiplied by the right hand side, which can be evaluated numerically in many ways. Note that the Green's function is independent of the right hand side.

5.1.1 Sturm-Liouville problem

It can be shown that a Sturm-Liouville (any heat problem will fall under this category) problem has a Green's function of the form:

$$G(x) = \begin{cases} -\dfrac{y_1(s)y_2(x)}{p(x)W[y_1, y_2](x)} & \text{if } 0 \le s \le x \\ -\dfrac{y_1(x)y_2(s)}{p(x)W[y_1, y_2](x)} & \text{if } x \le s \le 1 \end{cases} \tag{28}$$

Notice that equation 27 is indeed given by equation 28. Also note the symmetry of the Green's function: $G(x,s) = G(s,x)$.

5.1.2 Dirac Delta function

Another property of the Green's function is that it satisfies a particular differential equation, $\mathcal{L}(y) = \delta(s-x)$. If we verify this using Example 1, we see equation 27 is the solution to the differential equation:

$$-\frac{d^2y}{ds^2} = \delta(s-x) \tag{29}$$

$$\text{or, equivalently } -\frac{d^2y}{dx^2} = \delta(x-s) \tag{30}$$

Proof: To satisfy this, G_{ss} must satisfy the following properties (by definition of the Dirac delta function):

$$G_{ss} = 0 \text{ for } s \neq x \tag{31}$$

$$\int_0^1 G_{ss} ds = 1 \tag{32}$$

First condition:

$$G(x,s) = \begin{cases} s(1-x) & \text{if } 0 \le s \le x \\ x(1-s) & \text{if } x \le s \le 1 \end{cases}$$

$$-G_s(x,s) = \begin{cases} -1+x & \text{if } 0 \le s < x \\ x & \text{if } x < s \le 1 \end{cases}$$

$$-G_{ss}(x,s) = \begin{cases} 0 & \text{if } 0 \le s < x \\ 0 & \text{if } x < s \le 1 \end{cases}$$

Second condition:

$$\int_0^1 -G_{ss} ds = -(G_s(1) - G_s(0)) = -((-1+x) - x) = 1. \blacksquare \tag{33}$$

Continuing our exploration of the delta function, we find the Fourier series expansion for the delta function as:

$$\delta(x) = 1 + \sum_{n=1}^{\infty} 2\cos(2n\pi x), \quad \delta(s-x) = 1 + \sum_{n=1}^{\infty} 2\cos(2n\pi(s-x)) \tag{34}$$

Using Geometric series formulas and trig, we can find a closed form for the delta function, also known as the Dirichlet Kernel:

$$
\begin{aligned}
1+\sum_{n=1}^{N} 2\cos(2n\pi x) &= \sum_{-N}^{N} e^{2\pi n i x} \\
&= 1+\sum_{1}^{N}(e^{2\pi i x})^n + \sum_{1}^{N}(e^{-(2\pi i x)})^n \\
&= \frac{\sin((N+1/2)x)}{2\pi\sin(x/2)}
\end{aligned}
$$

5.1.3 Expanding the Green's function using Fourier series

We first begin with the Fourier terms with arbitrary coefficients, a_n and b_n, assuming the Green's function is in the form:

$$G(x,s) = a_0 + \sum_{n=1}^{\infty} a_n \cos(2n\pi s) + \sum_{n=1}^{\infty} b_n \sin(2n\pi s) \tag{35}$$

And we directly calculate the coefficients to be:

$$a_0 = \frac{-x^2}{2} + \frac{x}{2} \tag{36}$$

$$a_n = \frac{\cos(2n\pi x) - 1}{2n^2\pi^2} \tag{37}$$

$$b_n = \frac{\sin(2n\pi x)}{2n^2\pi^2} \tag{38}$$

If we want to verify the identity given in equation (30), we can take two derivatives of Green's function expansion and compare that with Fourier series expansion for $\delta(s-x)$.

Recall that the Fourier series expansion for the delta function is:

$$\delta(s-x) = 1 + \sum_{n=1}^{\infty} 2\cos(2n\pi(s-x)), \quad \delta(x) = 1 + \sum_{n=1}^{\infty} 2\cos(2n\pi x) \tag{39}$$

However, two derivatives of Green's function expansion is:

$$
\begin{aligned}
G_{ss} &= 2\sum \cos(2n\pi(s-x)) - 2\sum \cos(2n\pi s) \\
&= \delta(s-x) - \delta(s)
\end{aligned}
$$

This is because the Fourier series expansion is given for the *periodic extension* of the Green's function, which places a delta function at the origin in addition to x.

5.2 Example 2

In this example, we look at a problem with a slightly more complicated left hand side:

$$-(y'' + y') = f(x)$$

With the same boundary conditions as above, $y(0) = 0$, $y(1) = 0$, we get the Green's function to be:

$$G(x) = \begin{cases} \frac{\sin s \sin(1-x)}{sin1} & \text{if } 0 \le s \le x \\ \frac{\sin x \sin(1-s)}{sin1} & \text{if } x \le s \le 1 \end{cases}$$

The following method expands the previous two examples to solve the Laplacian in 2D. The Green's function in 2D will then have *two* target variables, x and y, and *two* source variables, which we will call ξ and η.

6 Boundary Element Method

The third method we use to attempt to solve the Dirichlet problem for a square is the Boundary Element Method. This method is particularly useful for irregular boundaries, where separation of variables and discretization becomes particularly difficult. The boundary element method, as we saw somewhat in the previous examples, converts the PDE into an integral equation, which can be discretized and solved with any integral approximation methods, like midpoint and endpoint approximations.

If we are given either the temperature, $\phi(x,y)$, or the heat flux, $\frac{\partial}{\partial n}\phi(x,y)$, (but not both) at each point of the boundary $c = \partial D$ of domain D, then the temperature in the domain is given by the boundary integral

$$\phi(\xi,\eta) = \oint_c \phi(x,y)\frac{\partial}{\partial n}\Phi(x,y,\xi,\eta) - \Phi(x,y,\xi,\eta)\frac{\partial}{\partial n}\phi(x,y)ds(x,y), \tag{40}$$

$$\Phi(x,y,\xi,\eta) = \frac{1}{4\pi}\ln((x-\xi)^2 + (y-\eta)^2), \tag{41}$$

where $\Phi(x,y,\xi,\eta)$ is the Green's function for the Laplace equation in 2D and the normal derivative $\frac{\partial}{\partial n}\Phi(x,y,\xi,\eta)$ is with respect to a unit normal vector at (x,y). This relation is derived using the divergence theorem and the fact that Φ is a fundamental solution to the 2D Laplace equation [2],

$$-\nabla^2\Phi(x,y,\xi,\eta) = \delta(x-\xi, y-\eta). \tag{42}$$

Our second integral relation is for points on the boundary. If (ξ,η) is on a smooth part of the boundary, then we have the following boundary integral equation,

$$\frac{1}{2}\phi(\xi,\eta) = \oint_c \phi(x,y)\frac{\partial}{\partial n}\Phi(x,y,\xi,\eta) - \Phi(x,y,\xi,\eta)\frac{\partial}{\partial n}\phi(x,y)ds(x,y). \tag{43}$$

6.1 Simple case: Square

Let us consider the Dirichlet problem for the Laplace equation on the unit square. Then we rewrite equation (43) as,

$$\oint_c \Phi(x,y,\xi,\eta)\frac{\partial}{\partial n}\phi(x,y)ds(x,y) = -\frac{1}{2}\phi(\xi,\eta) + \oint_c \phi(x,y)\frac{\partial}{\partial n}\Phi(x,y,\xi,\eta)ds(x,y), \tag{44}$$

where the unknown boundary values of $\frac{\partial}{\partial n}\phi(x,y)$ are on the left and the known boundary values of $\phi(x,y)$ are on the right. Now discretize the boundary by piecewise linear segments so that

$$c = \sum_{k=1}^{N} c_k,$$

and let $(\xi_m, \eta_m), m = 1 : N$ be the endpoints of the segments. Also let $\phi_m = \phi(\xi_m, \eta_m)$ be the known boundary values of the potential, and let $p_m \approx \frac{\partial}{\partial n}\phi(\xi_m, \eta_m)$, be the unknown boundary values of the potential normal derivative. Now we evaluate equation (44) for $(\xi, \eta) = (\xi_m, \eta_m)$, and replace the integral over c by the sum of integrals over the segments,

$$\sum_{k=1}^{N} \int_{c_k} \Phi(x, y, \xi_m, \eta_m) \frac{\partial}{\partial n}\phi(x, y) ds(x, y) = -\frac{1}{2}\phi_m + \sum_{k=1}^{N} \int_{c_k} \phi(x, y) \frac{\partial}{\partial n}\Phi(x, y, \xi_m, \eta_m) ds(x, y). \tag{45}$$

Now approximate the integral over c_k, assuming $\frac{\partial}{\partial n}\phi(x, y) = p_k$ and $\phi(x, y) = \phi_k$ are constant on c_k,

$$\sum_{k=1}^{N} F_1^k(\xi_m, \eta_m) p_k = -\frac{1}{2}\phi_m + \sum_{k=1}^{N} \phi_k F_2^k(\xi_m, \eta_m), \quad m = 1 : N, \tag{46a}$$

$$F_1^k(\xi_m, \eta_m) = \int_{c_k} \Phi(x, y, \xi_m, \eta_m) ds(x, y) \approx \Phi(x_k, y_k, \xi_m, \eta_m)\ell_k, \tag{46b}$$

$$F_2^k(\xi_m, \eta_m) = \int_{c_k} \frac{\partial}{\partial n}\Phi(x, y, \xi_m, \eta_m) ds(x, y) \approx \frac{\partial}{\partial n}\Phi(x_k, \eta_k, \xi_m, \eta_m)\ell_k, \tag{46c}$$

where (x_k, y_k) is the midpoint of the kth interval, and ℓ_k is the length of the kth interval. equation (46a) can be rewritten as a linear system $\mathbf{F}\vec{p} = \vec{\phi}$:

$$\begin{bmatrix} F_1^1(\xi_1, \eta_1) & \dots & F_1^N(\xi_1, \eta_1) \\ \vdots & & \vdots \\ F_1^1(\xi_N, \eta_N) & \dots & F_1^N(\xi_N, \eta_N) \end{bmatrix} \begin{bmatrix} p_1 \\ \vdots \\ p_N \end{bmatrix} = \begin{bmatrix} -\frac{1}{2}\phi_1 + \sum_{k=1}^{N} \phi_k F_2^k(\xi_1, \eta_1) \\ \vdots \\ -\frac{1}{2}\phi_N + \sum_{k=1}^{N} \phi_k F_2^k(\xi_N, \eta_N) \end{bmatrix} \tag{47}$$

Once all the $p_k s$ are known, we can compute the temperature at interior points (ξ, η) using equation (40):

$$\phi(\xi, \eta) = \sum_{k=1}^{N} [\phi_k F_2^k(\xi, \eta) - p_k F_1^k(\xi, \eta)]. \tag{48}$$

The domain is given by $D = \{(x, y) \in (0, L) \times (0, L)\}$. The boundary is given by 4 sides of a square. Each side is further divided into N segments, c_k. The length of each segment is $\ell = L/N$.

$$c = \sum_{k=1}^{4N} c_k$$

.

Tracing the boundary counterclockwise, the midpoints (where we evaluate F_1 and F_2) of each segment c_k are given by (x_k, y_k) and the end points (where we place the singularities of F_1 and F_2 of each segment c_m) are given by (ξ_m, η_m):

For $k = m = 1 : N, (x_k, y_k) = (\ell(k - 1/2), 0), (\xi_m, \eta_m) = (\ell k, 0)$

For $k = N + 1 : 2N, (x_k, y_k) = (L, \ell(k \mod 4 - 1/2)), (\xi_m, \eta_m) = (L, \ell k \mod 4)$

For $k = 2N + 1 : 3N, (x_k, y_k) = (L - \ell(k \mod 4 - 1/2), L), (\xi_m, \eta_m) = (L - \ell k \mod 4, L)$

For $k = 3N + 1 : 4N, (x_k, y_k) = (0, L - \ell(k \mod 4 - 1/2)), (\xi_m, \eta_m) = (0, L - \ell k \mod 4)$.

$$F_1^k(\xi_m, \eta_m) \approx \Phi(x_k, y_k, \xi_m, \eta_m)\ell, \quad F_2^k(\xi_m, \eta_m) \approx \frac{\partial}{\partial n}\Phi(x_k, \eta_k, \xi_m, \eta_m)\ell. \tag{49}$$

This is where we started to see the method fail. The matrix in equation (47) is ill-conditioned and not full rank. We should have stated more clearly what the objective was, to find the temperature on the interior. There is really no need to find the normal derivative on the boundary. Instead, we should try using an indirect boundary integral, as opposed to the direct method formulated above. The indirect boundary integral method would consist of finding a "charge density" function along the boundary, where the temperature in the interior is given by:

$$\phi(x, y, \xi, \eta) = \oint_c \frac{\partial}{\partial n}\Phi(x, y, \xi, \eta)\sigma(x, y)ds(x, y) \tag{50}$$

Where, when (x, y) is on the boundary, the relation is:

$$\phi(x, y, \xi, \eta) = \frac{1}{2}\sigma(\xi, \eta) + \oint_c \frac{\partial}{\partial n}\Phi(x, y, \xi, \eta)\sigma(x, y)ds(x, y). \tag{51}$$

This integral equation would provide a better conditioned matrix.

7 Conclusion

In this project we studied the heat equation in many different forms. We picked a particular problem, the steady state heat conduction problem on a finite square, and (attempted) to solve it in multiple ways. Each method had its own drawbacks and advantages. In the future, it would be interesting to compute the indirect boundary element integral method outlined in the previous section and compare it with results obtained using the finite difference method and the spectral method (Fourier series expansions). Another future goal would be considering more interesting domains, like a block-M as 3D printed on in a Smartscan experiment. Finally, coupling in elasticity to circle back to the powder bed fusion and warping issues in the 3D printing process.

References

[1] Keval S. Ramani , Chuan He , Yueh-Lin Tsai , Chinedum E. Okwudire. SmartScan: An intelligent scanning approach for uniform thermal distribution, reduced residual stresses and deformations in PBF additive manufacturing, Additive Manufacturing 52 (2022) 102643.

[2] Whye-Teong Ang. A Beginner's Course in Boundary Element Methods, Universal Publishers (2007).

[3] Joseph Fourier. The Analytical Theory of Heat, Translated by Alexander Freeman, Cambridge University (1822).

[4] Kenneth M Monks. Fourier's Heat Equation and the Birth of Modern Climate Science, MAA Convergence (February 2022).

[5] William E. Boyce, Richard C. Diprima, Douglas B. Meade. Elementary Differential Equations and Boundary Value Problems, 11th edition, Wiley (2017).